Daidalos-Cloud: PV Module Simulation Manual

Version: 2019-05-17

Authors: Malte R. Vogt, Lukas Brockmann, Oliver Lange
Robert Witteck, Timo Gewohn, Carsten Schinke

Contact us: daidalos@isfh.de

Table of content

1. Introduction to *Daidalos-Cloud*: PV Module Simulations

Daidalos[1] is a ray tracing framework originally developed for the purpose of simulating the optical properties of photovoltaic (PV) modules in their environment. It enables many different applications from ray tracing of building facades to ray tracing of solar cell texture elements. However, this manual focusses on one specific simulation type, PV Module simulations, which can be performed using the online interface of Daidalos, namely *Daidalos-Cloud*.

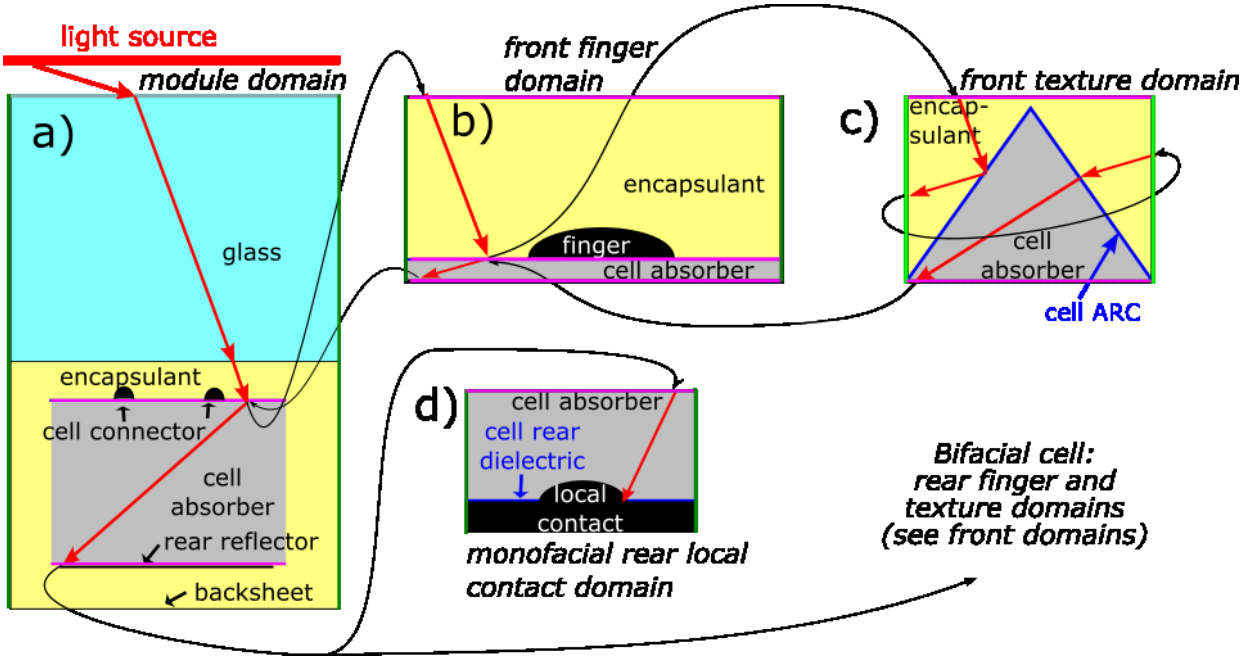

Figure 1 Multi-domain approach in Daidalos. a) Module domain containing the glass, encapsulation, cell interconnect ribbon (CIR), cells and back sheet. b) Front finger domain containing the front metal fingers. c) Front texture domain containing the pyramid texture with the cells front anti-reflection coating (ARC). d) Monofacial rear local contact domain containing the local contact, rear dielectric coating and a slice of the rear metallization.

In order to simulate the interaction of light with a PV module, not only light hitting the solar cells must be considered, but also light hitting the gaps between the solar cells. This can be achieved by using a multi-domain approach [2] as illustrated in *Figure 1*. In the multi-domain approach, the simulated geometry is split into several domains. Each domain contains one symmetry element (modeled in three dimensions) and appropriate boundary conditions to represent its periodic or random lateral repetition. In order to enable interaction between objects in different domains, there needs to be a way for the light rays to travel from one domain to another. From the perspective of the light ray, the way through the different domains needs to represent the path through a real PV module. Depending on the cell architecture, up to five domains are required

for a representation of a PV module. The first (top-level) domain is called “module domain”. It is irradiated by the light source and contains one solar cell and its surrounding components in the module. The second domain is the “front finger domain”. It contains the symmetry element surrounding one front finger. The third domain is the “front texture domain”. It contains the symmetry element of the surface texture and its surroundings. Depending on the cell architecture, a “rear texture domain” and a “rear finger domain” or “rear contact domain” are also used. Each of these domains apply periodic (dark green lines) or random (light green lines) boundary conditions at their side faces. In contrast, top and bottom faces of domains b)-d) are connecting the domains via surface effects (magenta lines) which shift light rays from one domain to another. For a more in-depth look of this approach or the implementation of the optical physics principles and equations please see [3].

In the following, we provide a manual for the use of this PV module simulation via the Daidalos-Cloud interface covering the in- and output options for the user.

2. Guide for *Daidalos-Cloud*: PV Module Simulations

In this chapter the procedure of running a ray tracing simulation using *Daidalos-Cloud* website to is presented. This chapter is split into three subchapters: Input parameters, materials used in simulations and evaluation of the simulated results.

2.1 Input parameters for *Daidalos-Cloud*: Module Simulations

The input parameters of *Daidalos-Cloud* can be varied to create a wide range of possible combinations of resulting in very different solar cells and modules. Tables 1 through 8 provide an overview of the input parameters of *Daidalos-Cloud*:

Table 1: Overview of cell configuration parameters

Table 2: Overview of cell dielectric parameters

Table 3: Overview of cell metallization parameters

Table 4: Overview of monofacial rear side domain *parameters*

Table 5: Overview of cell interconnect *ribbons parameters*

Table 6: Overview of module domain *parameters*

Table 7: Overview of glass-glass module parameters

Table 8: Overview of irradiation condition parameters

2.1.1 Cell configuration

Figure 2 shows the module simulation domain. It contains the glass, the encapsulation, cell interconnect ribbons, the cell, and the backsheet or rear glass.

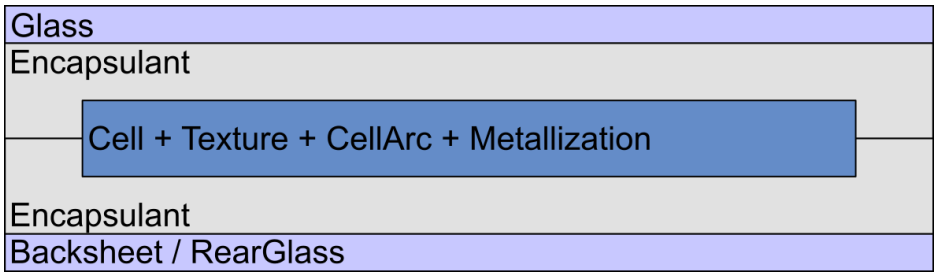

Figure 2: Example for the module domain for a Daidalos-Cloud PV module simulation

By switching the *CellonlySwitch* to true, it is possible to simulate a cell without a surrounding module. In *Figure 2* glass, encapsulants and backsheet or rear glass material will be set to air. The cell will be set to full square and the *InterCellGap* will be set to 0.1 µm and side boundaries will be set to act as perfect absorber. This option is especially useful for simulating the losses caused by the incorporation of a cell into a module.

The *BifacialcellSwitch* changes the cell between a bifacial and a monofacial cell structure. In case of a bifacial solar cell the full-area backside metallization is exchanged with a rear finger grid.

The *CellHasFrontTextureSwitch* and *CellHasRearTextureSwitch* change the front and rear surface of the cell between planar and a random pyramid texture (striped pyramids in Fig. 3). The *CellHasRearTextureSwitch* has only an effect if the *BifacialcellSwitch* is set to true.

The *CellSubstrateMaterial* defines the absorber material of the cell, typically silicon. Height and width of the cell are *CellWidth* and *CellHeight*, both in µm.

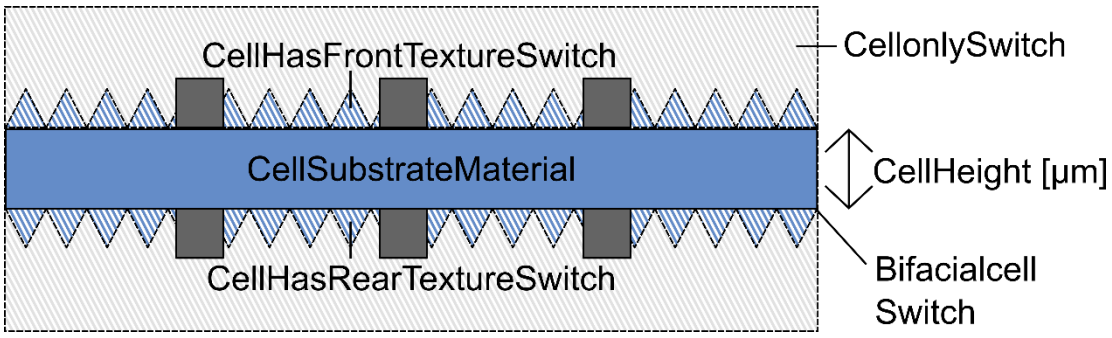

Figure 3: Side view of the cell.

The *PseudoSquareCellSwitch* sets the cell geometry to “pseudo-square”, if set to true and “full square”, if set false, as shown in Figure 4. For a pseudo-square cell the corners of the cell are cut off due to minimization of waste material by cutting a rectangular

shape out of a round wafer. If the cell is pseudo square the *PseudoSquareCellDiameter* is used to determine the cutoff at the corners of the cell.

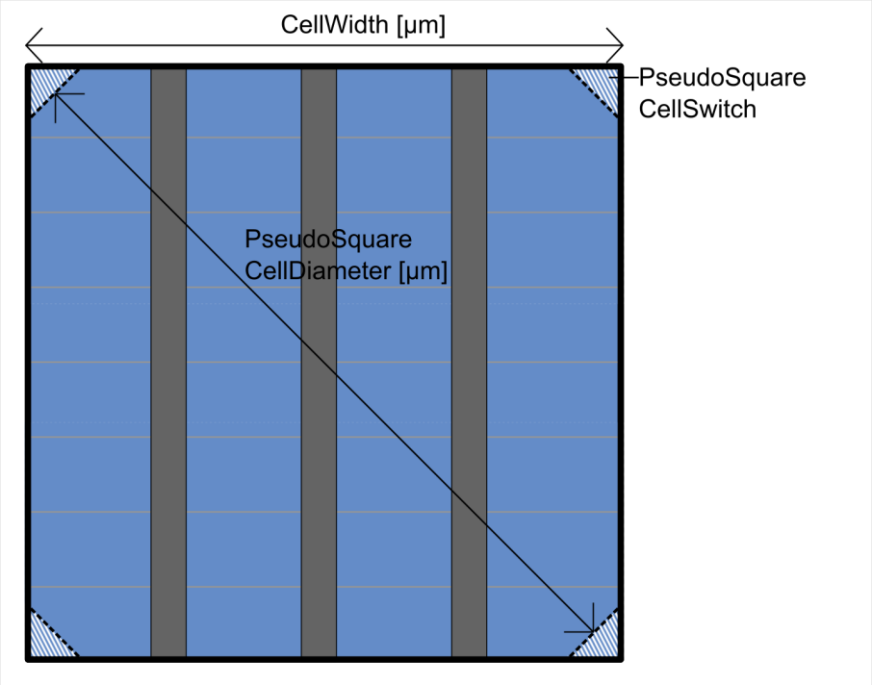

Figure 4: Top view of the solar cell.

Table 1: Overview of cell configuration parameters

Parameter	Unit	Min	Max	Default	Description
BifacialcellSwitch	bool	-	-	false	True = no full area backside metallization and rear finger domain present False = full area backside metallization and rear local contact domain present
CellonlySwitch	bool	-	-	false	True = Cell in air (all materials surrounding the cell are air) False= Cell in the module
PseudoSquareCellSwitch	bool	-	-	false	True = pseudo square solar cell False = full square solar cell
CellHasFrontTextureSwitch	bool	-	-	true	True = random pyramids on front side of solar cell

					False = planar front side of solar cell
CellHasRearTextureSwitch	bool	-	-	false	True = random pyramids on rear side of solar cell (only if BifacialcellSwitch=true) False = planar rear side of solar cell (only if BifacialcellSwitch=true)
PseudoSquareCellDiameter	µm	1	636396	210000	Diameter of the cell if pseudo square
CellHeight	µm	10	500	170	Solar cell thickness
CellWidth	µm	1	450000	156750	Solar cell edge length
CellSubstrateMaterial	String	-	-	Si_CS	Material of the solar cell substrate / absorber

2.1.2 Solar cell dielectric layers

On top and below the cell material are anti reflection coatings (ARC) to reduce the optical reflection losses of the cell or dielectric layers to reduce surface recombination. The ARC layers are on top of the planar or textured *CellSubstrateMaterial*. Every ARC material (*FrontArcMaterials* or *RearArcMaterials*) requires a corresponding thickness (*FrontArcThicknesses* or *RearArcThicknesses*). The layer with the higher number is always closest to the solar cell. Please note that these cell coating layers and the glass coating layers are the only layers, which consider interference. For a more in-depth look of the implementation of the optical physics principles please see [3].

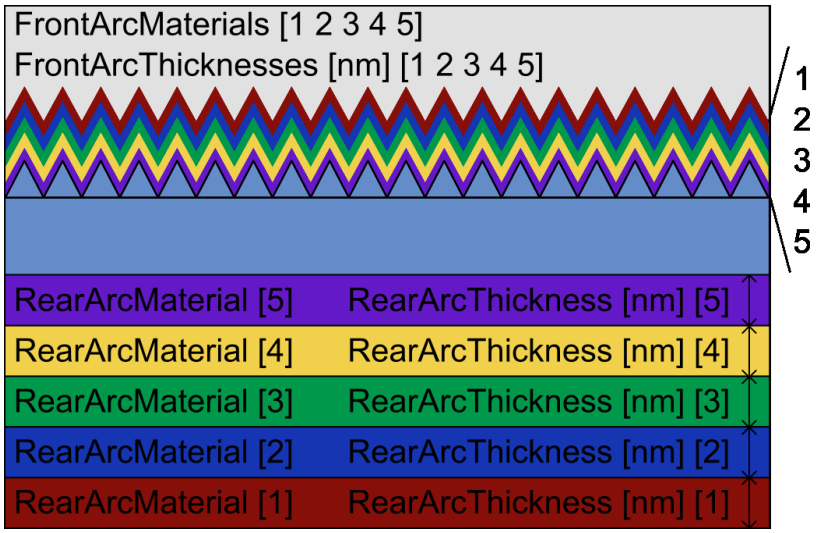

Figure 5: Configuration of dielectric coating layers.

Table 2: Overview of cell dielectric parameters

Parameter	Unit	Min	Max	Default	Description
FrontArcMaterials	String	zero layers	five layers	SiN209_TIFit	Front ARC materials
FrontArcThicknesses	nm	1	500	74	Front ARC thickness
RearArcMaterials	String	zero layers	five layers	SiN209_TIFit Al2O3	Rear ARC materials
RearArcThicknesses	nm	1	500	82 5	Rear ARC thickness

2.1.3 Cell metallization configuration

To save computation time in a Daidalos-Cloud simulation the cell fingers are in their own domain, which is shown in the cross section in Figure 6. The implemented cross section of the cell interconnect ribbons was experimentally determined in [4].There are five main parameters to adjust the settings of the fingers.

NumberOfFingers defines the number of front metal fingers of the cell. *FingerWidth* is the width at the base of the finger, while the *FingerHeight* equals the distance between the base and the top of the finger.

The optical properties are manipulated by *FingerMaterial* and *FrontFingerLambertianFactor*, a number between 0 and 1, where 0 equals 0% scattering (all reflections are specular) and 1 equals 100% scattering (all reflections are Lambertian).

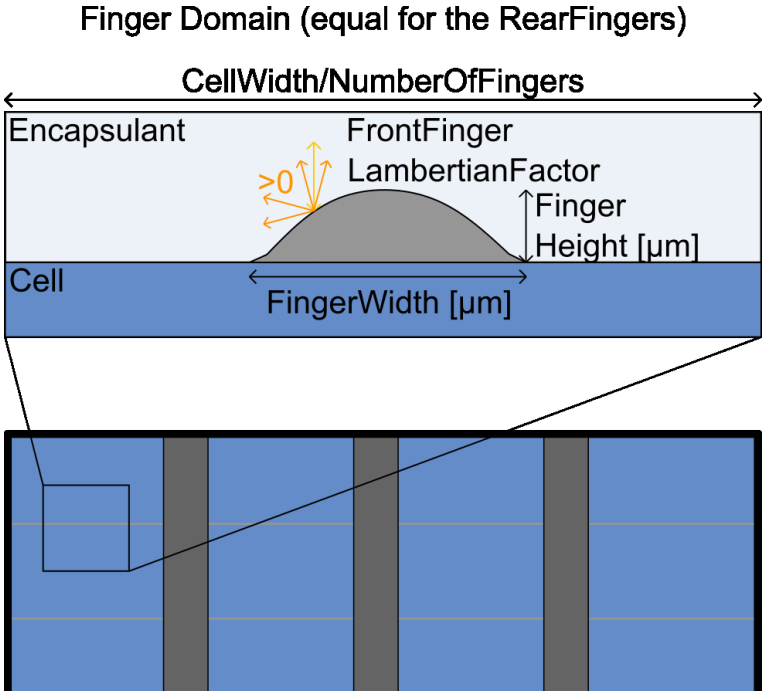

Figure 6: Schematic of the finger domain

If the cell is bifacial the rear metallization of the cell is also a number of fingers in their own domain. The same purpose is served with those parameters: *NumberOfRearFingers*, *RearFingerWidth*, *RearFingerHeight*, *RearFingerMaterial* and *RearFingerLambertianFactor*.

Table 3: Overview of cell metallization parameters

Parameter	Unit	Min	Max	Default	Description
NumberOfFingers	Integer	1	500	120	Number of front fingers
FingerWidth	µm	1	200	35	Width of front fingers
FingerHeight	µm	1	100	20	Height of front fingers
FingerMaterial	String	-	-	Ag	Material of front fingers
FrontFingerLambertianFactor	Float	0	1	0.8	Lambertian factor: Adjusting the scattering of the front fingers. 0 sets all reflections as specular. 1 sets all reflections as lambertian.
NumberOfRearFingers	Integer	1	500	160	Number of rear fingers
RearFingerWidth	µm	1	200	80	Width of rear fingers
RearFingerHeight	µm	1	100	20	Height of rear fingers
RearFingerMaterial	String	-	-	Al	Material of rear fingers
RearFingerLambertianFactor	Float	0	1	0.8	Lambertian factor: Adjusting the scattering of the rear fingers. 0 sets all reflections as specular. 1 sets all reflections as lambertian.

2.1.4 Monofacial cell rear side configuration

For monofacial cells the rear side metallization is a full area metal consisting of *CellRearMetalMaterial*. The electrical contacts are formed through LCO (local contact openings) in the dielectric layer where a metal contact with a local BSF (back surface field) is formed.

To save computation time in a Daidalos-Cloud simulation the local rear contacts are in their own domain. The local contact consists of the same material as the rear metal as shown in Figure 7. LCO width and LCO height characterize the rectangular shape of the LCOs. The width of the LCO domain equals *LCO distance* + *LCO width*. The extend of scattering is set by *LCO lambertian factor* for the LCOs and *Rear coating lambertian factor* for the interface of the rear metal. A number between 0 and 1, where 0 equals 0% scattering (all reflections are specular) and 1 equals 100% scattering (all reflections are Lambertian).

An “Al-BSF” type cell is create by setting the LCO height to zero and defining no RearArcMaterials.

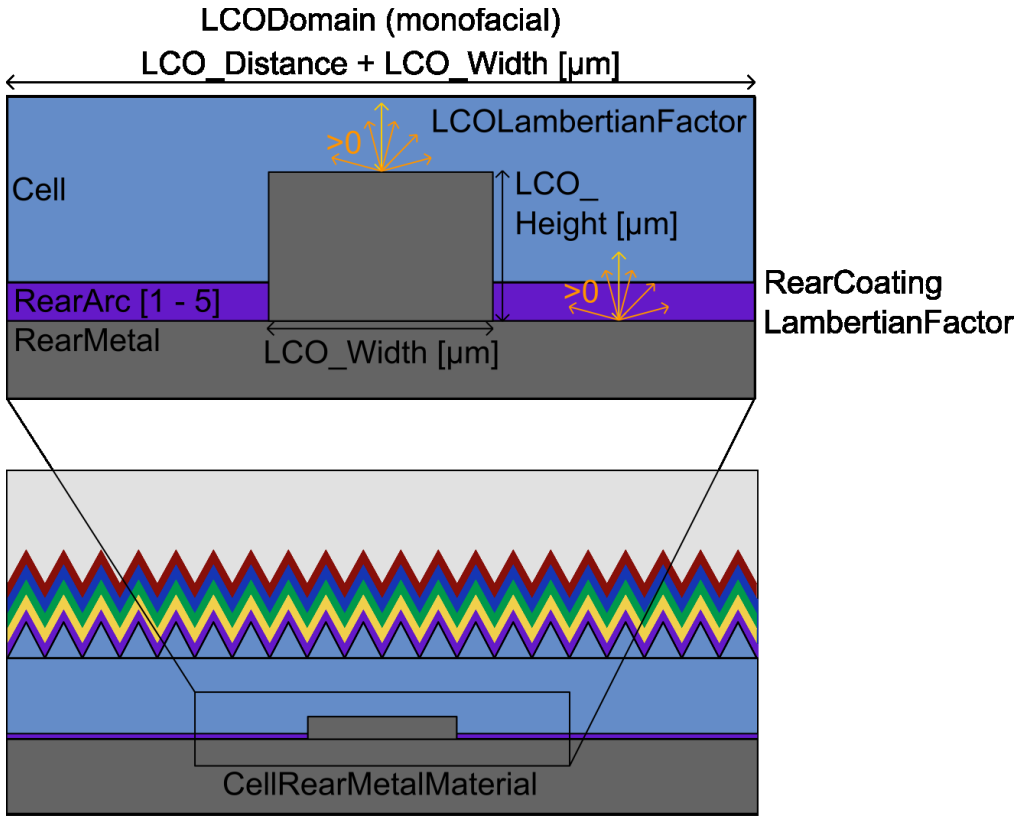

Figure 7: Monofacial cell rear side domain.

Table 4: Overview of monofacial rear side domain parameters

Parameter	Unit	Min	Max	Default	Description
CellRearMetalMaterial	String	-	-	AlSi_MaV	Rear side metallization material (monofacial)
Fehler! Verweisquelle konnte nicht gefunden werden.	µm	0	500	100	Width of local Al-BSF
Fehler! Verweisquelle konnte nicht gefunden werden.	µm	0	100	10	Height of local Al-BSF
LCO distance	µm	0	156750	900	Distance between Al-BSFs
LCO lambertian factor	Float	0	1	1	Lambertian factor. Adjusting the scattering of the local Al-BSFs. 0 sets all reflections as specular. 1 sets all reflections as lambertian.
Rear coating lambertian factor	Float	0	1	0.7	Lambertian factor. Adjusting the scattering of the rear side where no (local) Al-BSFs . 0 sets all reflections as specular. 1 sets all reflections as lambertian.

2.1.5 Cell interconnect ribbon configuration

The electrical connection between different cells is enabled by cell interconnect ribbons. The implemented cross section of the cell interconnect ribbons was experimentally determined in [5].

The number, width, height and material of the cell interconnect ribbons is set by *NumberOfInterconnectors* *InterconnectorWidth,* *InterconnectorHeight* and *InterconnectorMaterial*. The length of the cell interconnect ribbons always equals the cells' width.

The extend of scattering is set by *InterconnectorLambertianFactor*, a number between 0 and 1, where 0 equals 0% scattering (all reflections are specular) and 1 equals 100% scattering (all reflections are Lambertian).

All parameters for the cell interconnect ribbons s apply on the rear side of the cell except for *NumberOfRearInterconnectors*. It is possible to have different numbers of cell interconnect ribbons on top and below the bottom.

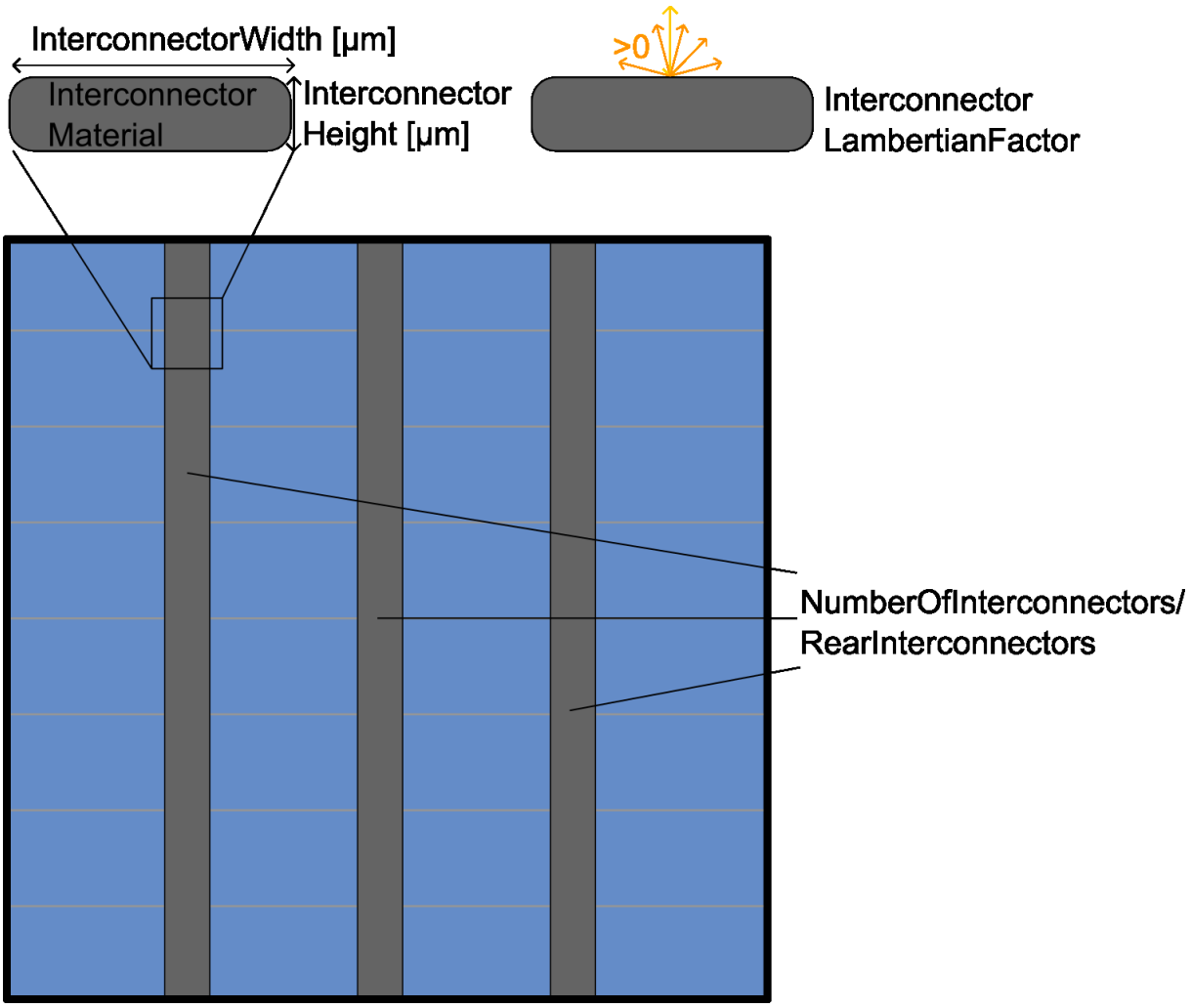

Figure 8: Cell interconnect ribbons above and below the cell.

Table 5: Overview of cell interconnect ribbons parameters

Parameter	Unit	Min	Max	Default	Description
NumberOf Interconnectors	Integer	0	50	5	Number of front cell interconnect ribbons
NumberOfRear Interconnectors	Integer	0	50	5	Number of rear cell interconnect ribbons
InterconnectorWidth	µm	1	3000	1000	Width of the cell interconnect ribbons
InterconnectorHeight	µm	1	500	200	Height of the cell interconnect ribbons
InterconnectorMaterial	String	-	-	Sn62.5Pb 36Ag1.5 (solder alloy [5])	Material of the cell interconnect ribbons
Interconnector LambertianFactor	Float	0	1	0.2	Lambertian factor. Adjusting the scattering of the cell interconnect ribbons. 0 sets all reflections as specular. 1 sets all reflections as lambertian.

2.1.6 Module domain parameters

This section allows the user to manipulate the module components surrounding the cell. Figure *9* shows cross-section view of the module domain with the available input parameters.

The top medium of the module typically the glass can be defined by the following two parameters the material "*GlassMaterial"* and thickness "*GlassHeight"* in µm. There can be a thin film coating (e.g. an ARC) with up to five layers on top of the glass. The ARC coating are up to five materials defined in *GlassArcMaterials* with the thicknesses of *GlassArcThicknesses*. The layer with the higher number is always the closer to the glass layer.

On top and below the cell are two layer typically the encapsulation: *EncapsulantMaterialAboveCell* and *EncapsulantMaterialBelowCell*. Those materials also fill the gaps between the cells and connect to each other in the middle of the cell height. The encapsulant thicknesses are *EncapsulantHeightAboveCell* measured from the bottom of "GlassMaterial" to the top of the cell absorber and *EncapsulantHeightBelowCell* measured from the backsheet to the "CellRearMetalMaterial"(if the cell is monofacial) or the bottom of the cell absorber (if the cell is bifacial). The material between the cell is internally calculated based on the *CellHeight* and the height of the "CellRearMetalMaterial" (which is 20µm and currently nonadjustable on daidalos-cloud.de).

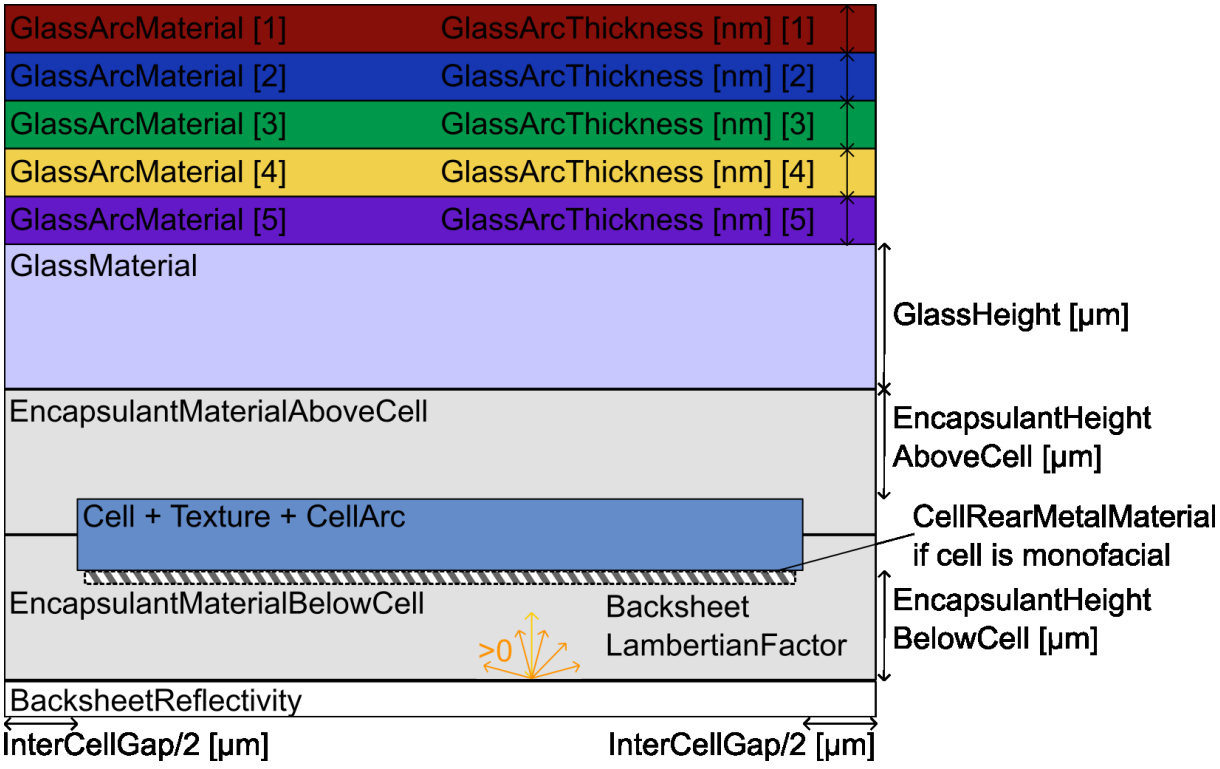

Figure 9 Schematic of a monofacial module.

The cell to cell spacing is called *InterCellGap* it determines the distance between the cell side and the periodic boundary conditions as shown in Figure *9*. The width of the encapsulants, the glass and the backsheet is equal to *InterCellGap* + *CellWidth* in the basic online version without advanced parameters.

The backsheet at the rear of the PV module reflects large portions of the incident light back to the cell. The parameter *BacksheetReflectivity* sets the spectrally resolved reflectance of the backsheet from an input file. All rays not reflected by the backsheet is assumed to be absorbed by the backsheet. The scattering of the backsheet can be adjusted by the *BacksheetLambertianFactor*, a number between 0 and 1, where 0 equals 0% scattering (all reflections are specular) and 1 equals 100% scattering (all reflections are Lambertian).

Table 6: Overview of module domain parameters

Parameter	Unit	Min	Max	Default	Description
InterCellGap	µm	0.1	50000	2000	Distance between two cells
GlassHeight	µm	1	10000	3200	Thickness of the front side glass
GlassMaterial	String	-	-	Glass_Fe_0005_M0	Material of the front side glass
GlassArcMaterials	String	-	-	GlasARC_MaV	Glass ARC materials
GlassArcThicknesses	nm	1	500	115	Glass ARC thicknesses
EncapsulantHeight AboveCell	µm	1	5000	400	Thickness of the encapsulant above the cell
EncapsulantHeight BelowCell	µm	1	5000	400	Thickness of the encapsulant below the cell
EncapsulantMaterial AboveCell	String	-	-	EVA_UVT	Material of the encapsulant above the cell
EncapsulantMaterial BelowCell	String	-	-	EVA_UVT	Material of the encapsulant below the cell
BacksheetReflectivity	String	-	-	Backsheet_PYE_DissInEVA	File with backsheet reflectance
Backsheet LambertianFactor	-	0	1	0.95	Lambertian factor of the backsheet

2.1.7 Glass-glass module configuration

A bifacial module is simulated by setting the *GlassGlassModuleSwitch* to true, which disables the backsheet and replaces it with a rear glass layer. *RearGlassMaterial* sets the material of this layer and the *RearGlassHeight* sets thickness of the layer. *RearGlassArcMaterials* and *RearGlassArcThicknesses* adjust a thin film coating with up to five layers on the bottom of the glass-glass module. The parameters for the encapsulation and the front glass are described in section 2.1.6.

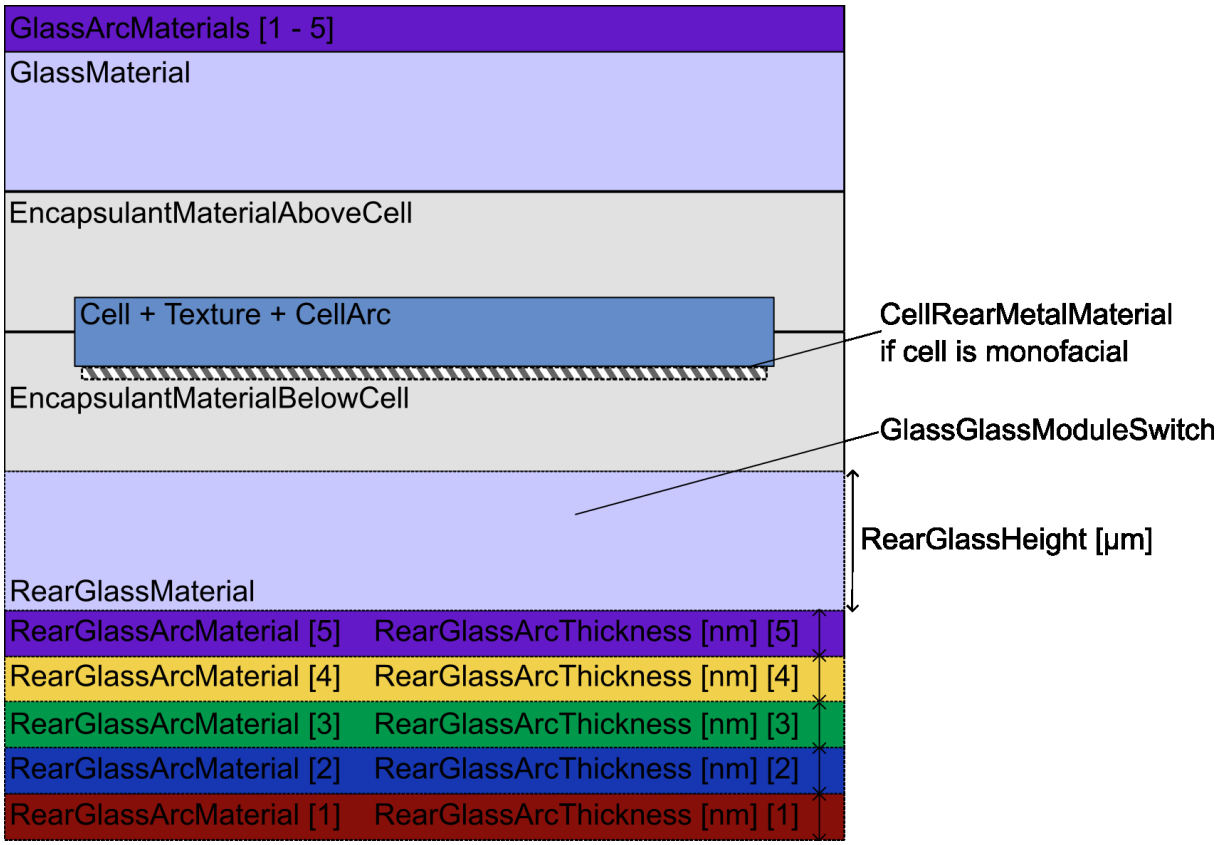

Figure 10: Schematic of glass on the rear side for a bifacial module

Table 7: Overview of glass-glass module parameters

Parameter	Unit	Min	Max	Default	Description
GlassGlassModuleSwitch	bool	-	-	false	True = Glass-glass module False = Module with backsheet
RearGlassHeight	µm	1	10000	2000	Thickness of the rear side glass
RearGlassMaterial	String	-	-		Material of the rear side glass
RearGlassArcMaterials	String	-	-	GlasARC_MaV	Rear glass ARC materials
RearGlassArcThicknesses	nm	0	500	115	Rear glass ARC thicknesses

2.1.8 Irradiation conditions

An area light source just above the front glass emits the rays for the simulation. For the basic online version, the simulated wavelength interval is always 300-1200 nm. The light sources spectral resolution is adjusted via the parameter *WavelengthStep*, which sets the difference between two simulated wavelengths. *PhotonsperWavelength* sets the number of rays simulated for each wavelength. Increasing the number of rays increases the computation time and reduces the statistical uncertainty. The *IncidentAngleInDegree* sets the angle of incidence for the incoming rays relative to the normal of the module front glass. The rotation axis is parallel to the cell interconnect ribbons.

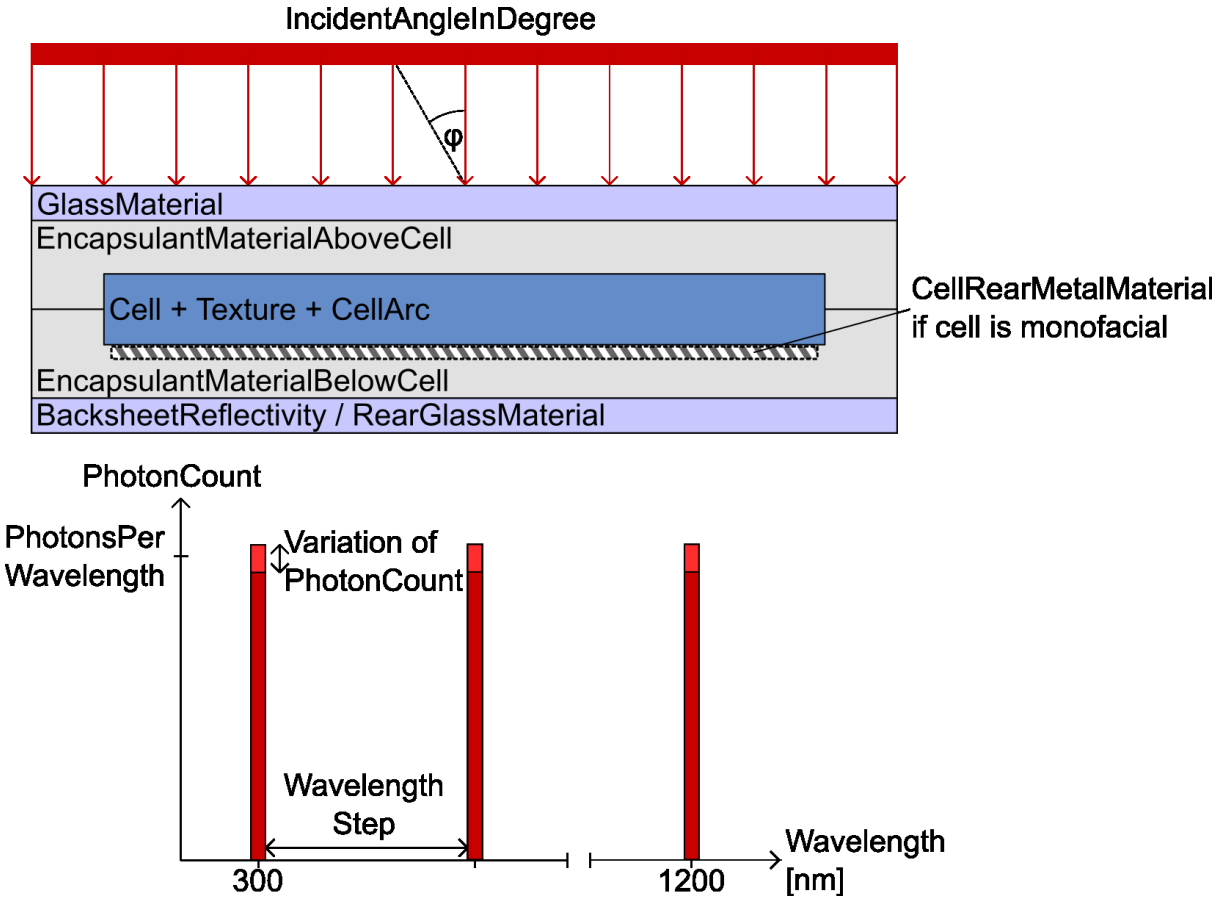

Figure 11: Area light source in Daidalos.

By switching the *UseDayLightSourceSwitch* to true the light source will be set to a daylight source: A light source with a mean spectrally resolved annual daylight distribution results for the full celestial hemisphere, which we partition into solid-angle intervals of 5° azimuth and 5° altitude (Figure 12). Each of these intervals contains its own spectral distribution for diffuse and direct light. We utilize an in-house developed mean annual daylight model [6][3] which uses irradiances measured over 14 years (1992 – 2006) in Hamelin, Germany.

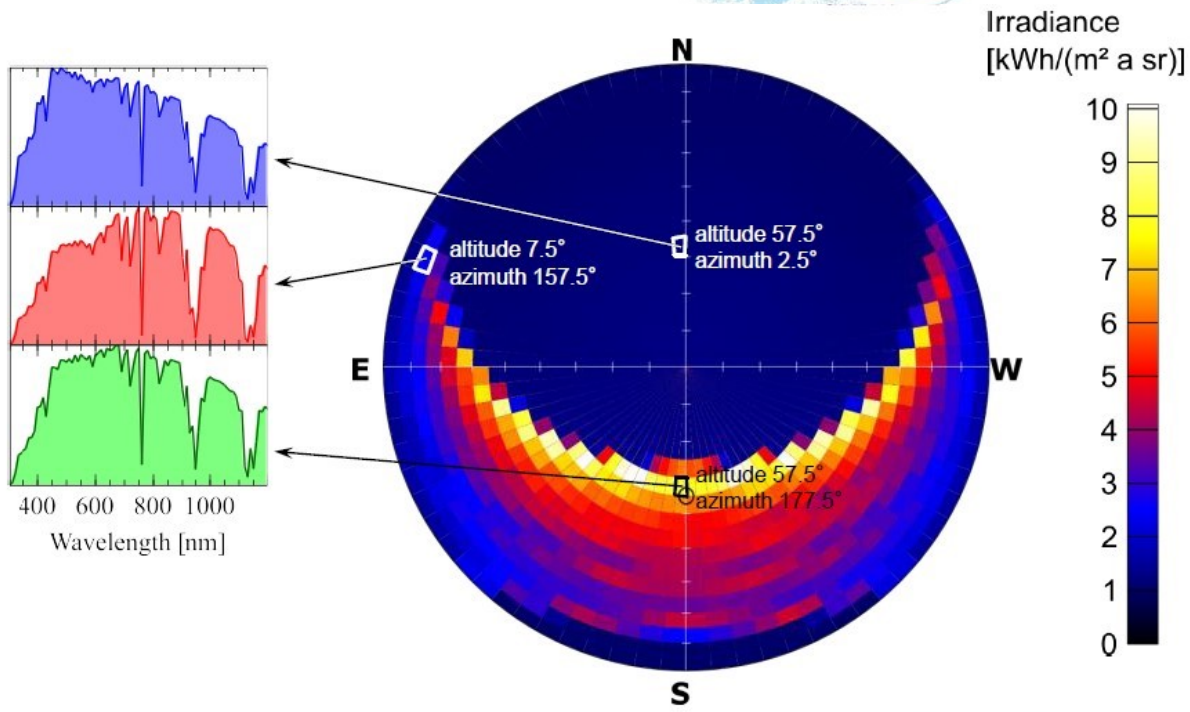

Figure 12: The mean annual daylight distribution partitions the celestial hemisphere into solid-angle intervals of 5° azimuth and 5° altitude. Each of these intervals contains its own spectral distribution of diffuse and direct light.

Table 8: Overview of irradiation condition parameters

Parameter	Unit	Min	Max	Default	Description
WavelengthStep	nm	5	100	10	Difference between wavelengths
PhotonsperWavelength	Integer	1	10000	5000	Number of rays per wavelength
UseDayLightSourceSwitch	bool	-	-	false	True = Mean annual light source is used False= Regular area light source is used
IncidentAngleInDegree	degree	0	89.9	0	Incident angle relative to with the rotation axis being parallel to the cell interconnect ribbons (only for regular light source)

2.2 Materials for simulations

In this chapter a brief overview of the materials used in simulations and their common purpose is shown. A lot of different materials are required in order to accurately model the resulting module.

Material files end with the file extension ".mat" to indicate its material properties. A material file consists of a table with a wavelength-dependent complex refractive index. The complex refractive index is compounded of a real part *n* and an imaginary part *k*. It is used to determine the probability of reflection, transmission and absorption of the rays of the corresponding wavelength in every material or at the interfaces between two materials.

The *BacksheetReflectivity* is given as a ".ref" file to state its reflection properties. A reflectivity file consists of a table with a wavelength-dependent reflection probability.

2.2.1 Cell absorber and cell dielectric layer materials

The following materials are commonly used as cell absorber material or cell dielectric layer:

Table 9: Materials for solar cell absorber and cell dielectric layers

Path	Purpose	Wavelength range[nm]	Description	Source
materials/ Si_CS.mat	Substrate/ Absorber	250 – 1700	*p*-type Czochralski grown monocrystalline silicon	[7] for k [8] for n
materials/ SiN191_TlFit.mat	Cell ARC/ Passivation	250 – 1700	Silicon nitride with *n* = 1.91 at 633 nm	[8]
materials/ SiN209_TlFit.mat	Cell ARC/ Passivation	250 – 1700	Silicon nitride with *n* = 2.09 at 633 nm	[8]
materials/ SiN213_TlFit.mat	Cell ARC/ Passivation	250 – 1700	Silicon nitride with *n* = 2.13 at 633 nm	[8]
materials/ Al2O3.mat	Cell ARC/ Passivation	300 – 1200	Aluminum oxide on shiny-etched samples	[9]
materials/ SiO2.mat	Cell ARC/ Passivation	300 – 1200	Silicon oxide	[10]
materials/ ZnOAl_TW.mat	Cell ARC/ Passivation	250 – 1690	Zinc oxide and aluminum layer	[11]
materials/ ITO.mat	Cell ARC/ Passivation	300 – 1200	Indium tin oxide	[12]

2.2.2 Cell metallization materials

The following materials are commonly used to model the cell metallization conducting the electrical currents:

Table 10: Cell metallization materials

Path	Purpose	Wavelength range[nm]	Description	Source
materials/ Ag.mat	Front Finger	300 – 1200	Silver for metal contacts	[10]
materials/ Al.mat	Rear Finger; BSF	300 – 1200	Aluminum for metal contacts	[13]
materials/ AlSi_MaV.mat	Al-BSF	250 – 1700	Aluminum silicon eutectic for BSF	[8]
materials/ Cu.mat	Wires	207 – 12400	Copper for metal contacts	[14]
materials/ Cu_JC.mat	Wires	188 – 1937	Copper for metal contacts	[15]
materials/ Sn62.5Pb36Ag1.5.mat	Cell interconnect ribbons	241 – 1695	Solder for cell interconnect ribbons	[5]

2.2.3 Glass and glass ARC materials

The glass the top layer of the module offers protection against weather and mechanical stress. Float glass with low iron concentration is commonly used as a glass for PV modules since iron is the main absorber in the glass. Daidalos-Cloud uses a semi-empirical model [16] to link a specific iron weight concentration to the extinction coefficient of the glasses. M0 indicates, that in this model all the absorption is caused by the Fe. In the M1 model Fe is responsible for all the absorption above the noise level[16].

Table 11: Glass and glass ARC materials

Path	Purpose	Wavelength range[nm]	Description	Source
materials/GlassFe/ Glass_Fe_0_M0.mat	Glass	240 – 1700	Float glass with 0% iron content (Fe_2O_3 wt%) according to Model 0	[16]
materials/GlassFe/ Glass_Fe_0_M1.mat	Glass	240 – 1700	Float glass with 0% iron content (Fe_2O_3 wt%) according to Model 1	[16]
materials/GlassFe/ Glass_Fe_00001_M0.mat	Glass	240 – 1700	Float glass with 0.0001 % iron content (Fe_2O_3 wt%) according to Model 0	[16]
materials/GlassFe/ Glass_Fe_00001_M1.mat	Glass	240 – 1700	Float glass with 0.0001 % iron content (Fe_2O_3 wt%) according to Model 1	[16]
materials/GlassFe/ Glass_Fe_0001_M0.mat	Glass	240 – 1700	Float glass with 0.001 % iron content (Fe_2O_3 wt%) according to Model 0	[16]
materials/GlassFe/ Glass_Fe_0001_M1.mat	Glass	240 – 1700	Float glass with 0.001 % iron content (Fe_2O_3 wt%) according to Model 1	[16]
materials/GlassFe/ Glass_Fe_001_M0.mat	Glass	240 – 1700	Float glass with 0.01 % iron content (Fe_2O_3 wt%) according to Model 0	[16]
materials/GlassFe/ Glass_Fe_001_M1.mat	Glass	240 – 1700	Float glass with 0.01 % iron content (Fe_2O_3 wt%) according to Model 1	[16]

materials/GlassFe/ Glass_Fe_01_M0.mat	Glass	240 – 1700	Float glass with 0.1 % iron content (Fe_2O_3 wt%) according to Model 0	[16]
materials/GlassFe/ Glass_Fe_01_M1.mat	Glass	240 – 1700	Float glass with 0.1 % iron content (Fe_2O_3 wt%) according to Model 1	[16]
materials/GlassFe/ Glass_Fe_0005_M0.mat	Glass	240 – 1700	Float glass with 0.005 % iron content (Fe_2O_3 wt%) according to Model 0	[16]
materials/GlassFe/ Glass_Fe_0005_M1.mat	Glass	240 – 1700	Float glass with 0.005 % iron content (Fe_2O_3 wt%) according to Model 1	[16]
materials/GlassFe/ Glass_Fe_005_M0.mat	Glass	240 – 1700	Float glass with 0.05 % iron content (Fe_2O_3 wt%) according to Model 0	[16]
materials/GlassFe/ Glass_Fe_005_M1.mat	Glass	240 – 1700	Float glass with 0.05 % iron content (Fe_2O_3 wt%) according to Model 1	[16]
materials/ PMMA.mat	Glass	240 – 1700	Acrylic glass	[11]
materials/ GlasARC_MaV.mat	Glass ARC	250 – 1700	Anti-reflection coating for glass	[8]
materials/ AF2400.mat	Glass ARC	300 – 1200	Teflon	[17] [18]
materials/ SiO2_1_11.mat	Glass ARC	300 – 1200	Silicon oxide with 78.9 % porosity	[19]
materials/ SiO2_1_15.mat	Glass ARC	300 – 1200	Silicon oxide with 70.9 % porosity	[19]
materials/ SiO2_1_25.mat	Glass ARC	300 – 1200	Silicon oxide with 49.7 % porosity	[19]
materials/ SiO2_1_28.mat	Glass ARC	300 – 1200	Silicon oxide with 43.0 % porosity	[19]
materials/ SiO2_1_33.mat	Glass ARC	300 – 1200	Silicon oxide with 31.5 % porosity	[19]
materials/ MgF2.mat	Glass or Cell ARC	300 – 1200	Magnesium fluoride	[10]

2.2.4 Encapsulation materials

Encapsulants are typically polymers. The real part of the refractive index *n* should be matched with the glass, while imaginary part of the refractive index *k* should be as close to zero as possible.

Table 12: Encapsulation materials

Path	Purpose	Wavelength range[nm]	Description	Source
materials/ air.mat	ENC	-	$n = 1$; $k = 0$ for every wavelength	-
materials/ EVA_UVA.mat	ENC	250 – 2500	UV- absorbing ethylene vinyl acetate	[20]
materials/ EVA_UVT.mat	ENC	250 – 2500	UV-transparent ethylene vinyl acetate	[20]
materials/ Silicone.mat	ENC	200 – 1600	Liquid UV-transparent silicone	[21]
materials/ Silicone_UVT.mat	ENC	250 – 2500	Solid UV-transparent silicone	[8]
materials/ SiliconeDCC201.mat	ENC	200 – 1600	Silicone with $n = 1.403$ at 633 nm	[22]
materials/ SiliconeDCC203.mat	ENC	200 – 1600	Silicone with $n = 1.468$ at 633 nm	[22]
materials/ SiliconeDCC205.mat	ENC	200 – 1600	Silicone with $n = 1.549$ at 633 nm	[22]

2.2.5 Backsheets

Backsheets are used in monofacial modules to reflect or scatter the light back to the absorber. They should offer a high reflectivity and low absorption and transmission. In the Daidalos-Cloud module ray tracer the backsheet is implemented as a reflection probability at the bottom of the solar module, thus the files listed in Table *13* contain hemispherical reflectance and not refractive indexes as all other tables in this section.

Table 13: Backsheets

Path	Purpose	Wavelength range[nm]	Description	Source
materials/ Backsheet_PYE_DissInAir.ref	Back-sheet	300 – 1200	White backsheet in air	[8]
materials/ Backsheet_PYE_DissInEVA.ref	Back-sheet	300 – 1200	White backsheet in EVA	[8]
materials/ BacksheetR0.ref	Back-sheet	300 – 2000	Backsheet with 0% reflectance	-
materials/ BacksheetR100.ref	Back-sheet	300 – 2000	Backsheet with 100% reflectance	-

2.3 Post processing of simulation results

The outputs of the simulation are presented in two diagrams and an excel sheet. The excel sheet contain four tables: The raw simulation data, the overview, the spectral information and the loss overview.

The raw data – the direct output of the simulation is shown in the tab “SimulationData” of the excel sheet “Simulationdata_[date]_[time].xls”, where date and time are set to the start of the simulation. Each column represents a cause of termination of the simulated rays, except for column A and column B. Column A shows the corresponding wavelength of the row. B shows the total number of simulated photons for the wavelength in column A. The names of the columns are designated by the loss mechanism: “A_[X]” means the ray was absorbed by X. “R_[X]” indicates a loss by reflection, causing the photon to leave the simulated area upwards. “Transmission” is only mentioned in bifacial modules and counts the number of photons leaving the simulated module through the rear glass.

In the tab “Overview”, on top of the table the Jsc_Cell and the Jsc_total are presented. Jsc_Cell is the output of the module based on the AMG 1.5 G spectrum and the collection efficiency of the semiconductor. For the area dependency the current was divided $(CellWidth + InterCellGap)^2$, thus multiplying it with the module area results in a current. The maximum possible output is Jsc_total and represents a module with optical losses equal to zero and a collection efficiency of 100% for the absorber with an AMG 1.5 G spectra.

The input parameters are also summarized in the tab “Overview”. The user can inspect the input parameters written down in order to find mistakes and redo a simulation with other parameters, if needed. On the list of input parameters are additional parameters not mentioned in the manual. Those parameters are set to defaults to create a module as presented in the chapters before. Those experimental parameters are available in the premium edition of Daidalos-Cloud to enable an even further customization of the simulated module.

The “Spectral information” tab is a wavelength-by-wavelength evaluation of module properties. An illustration of this sheet is presented by the “ART diagram.pdf” shown in Figure 13. It contains the spectrally resolved absorption of the cell (black, A_{cell}), the reflectance(red, R_{front}), transmission(blue T_{rear}) and parasitic absorption(green A_{mod}) of the module as well as their uncertainty.

The “Spectral information” tab also contains spectrum and the collection efficiency used for the calculation of the short circuit current.

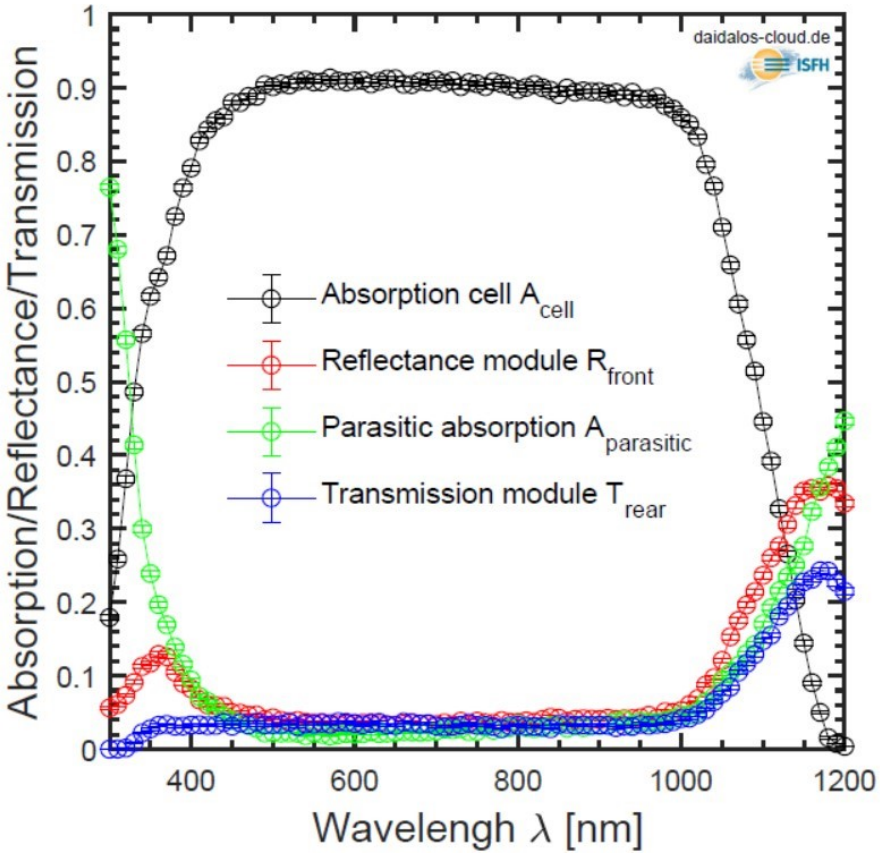

Figure 13: ART diagram contains the spectrally resolved absorption of the cell, the reflectance, transmission and parasitic absorption of the module as well as their uncertainty.

The “Loss overview” lists the optical loss mechanism of the module. The values are given in terms of photo generation current in [mA/cm²] and as the fraction of the losses in [%]. A visualization of this sheet is the diagram in “Loss fractions diagram.pdf” an example is shown in Figure *14* below.

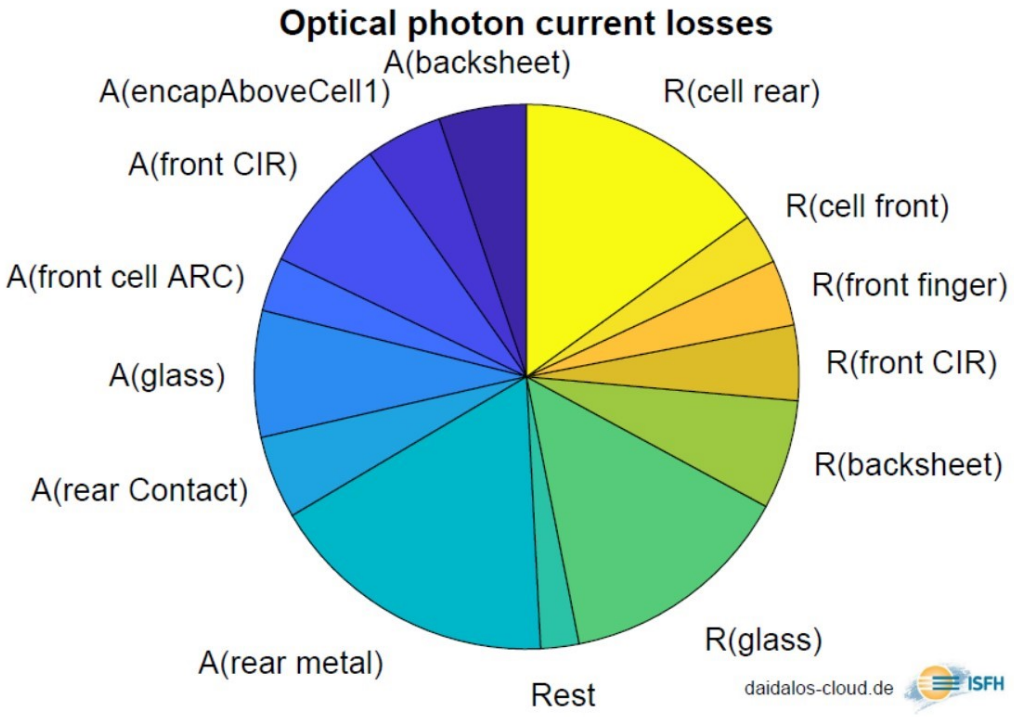

Figure 14: Loss fractions diagram for a simulated module.

3. References

[1] H. Holst *et al.*, “Application of a new ray tracing framework to the analysis of extended regions in Si solar cell modules,” *Energy Procedia*, vol. 38, pp. 86–93, 2013.

[2] M. Winter, M. R. Vogt, H. Holst, and P. P. Altermatt, “Combining structures on different length scales in ray tracing: analysis of optical losses in solar cell modules,” *Opt. Quantum Electron.*, vol. 47, no. 6, pp. 1373–1379, 2015.

[3] C. Schinke, M. R. Vogt, and K. Bothe, “Optical Modeling of Photovoltaic Modules with Ray Tracing Simulations,” in *Photovoltaic Modeling Handbook*, 2018, pp. 27–92.

[4] R. Witteck *et al.*, “Optimizing the Solar Cell Front Side Metallization and the Cell Interconnection for High Module Power Output,” *Energy Procedia*, vol. 92, pp. 531–539, Aug. 2016.

[5] H. Holst *et al.*, “Increased Light Harvesting by Structured Cell Interconnection Ribbons: An Optical Ray Tracing Study Using a Realistic Daylight Model,” *Energy Procedia*, vol. 92, pp. 505–514, 2016.

[6] M. Winter, H. Holst, M. R. Vogt, and P. P. Altermatt, “Impact of realistic illumination on optical losses in Si solar cell modules compared to standard testing conditions,” in *31st EU PVSEC*, 2015, pp. 1869–1874.

[7] C. Schinke *et al.*, “Uncertainty analysis for the coefficient of band-to-band absorption of crystalline silicon,” *AIP Adv.*, vol. 5, no. 6, p. 067168, 2015.

[8] M. R. Vogt, “Development of Physical Models for the Simulation of Optical Properties of Solar Cell Modules,” Leibniz University Hannover, 2015.

[9] “Aluminium-Oxide (Al2O3) measured at ISFH by Florian Werner.” .

[10] E. D. Palik, *Handbook of Optical Constants of Solids*. Academic Press Inc., 1985.

[11] R. Brendel *et al.*, “High Temperature Annealing of ZnO:Al on Passivating POLO Junctions: Impact on Transparency, Conductivity, Junction Passivation, and Interface Stability,” *IEEE J. Photovoltaics*, vol. 9, no. 1, pp. 89–96, 2018.

[12] “Indium-Tinn-Oxide(ITO) measured at ISFH by Nicole Ehrmann.” .

[13] E. Shiles, T. Sasaki, M. Inokuti, and D. Y. Smith, “Self-consistency and sum-rule tests in the Kramers-Kronig analysis of optical data: Applications to aluminum,” *Phys. Rev. B*, vol. 22, no. 4, pp. 1612–1628, 1980.

[14] A. D. Rakić, A. B. Djurišić, J. M. Elazar, and M. L. Majewski, “Optical properties of metallic films for vertical-cavity optoelectronic devices,” *Appl. Opt.*, vol. 37, no. 22, p. 5271, 1998.

[15] P. B. Johnson Christy, R. W., “Optical Constants of the Noble Metals,” vol. 1318, no. 1970, pp. 4370–4379, 1972.

[16] M. R. Vogt *et al.*, “Measurement of the Optical Constants of Soda-Lime

Glasses in Dependence of Iron Content and Modeling of Iron-Related Power Losses in Crystalline Si Solar Cell Modules," *IEEE J. Photovoltaics*, vol. 6, no. 1, pp. 111–118, 2016.

[17] J. H. Lowry, J. S. Mendlowitz, and N. S. (Mani) Subramanian, "Optical characteristics of Teflon AF fluoroplastic materials," *Opt. Eng.*, vol. 31, no. 9, p. 1982, 1992.

[18] M. K. Yang, "Optical properties of Teflon® AF amorphous fluoropolymers," *J. Micro/Nanolithography, MEMS, MOEMS*, vol. 7, no. 3, p. 033010, 2008.

[19] S. Yang and Y. Zhang, "Spectroscopic ellipsometry investigations of porous SiO2 films prepared by glancing angle deposition," *Surf. Interface Anal.*, vol. 45, no. 11, pp. 1690–1694, 2013.

[20] M. R. Vogt *et al.*, "Optical constants of UV transparent EVA and the impact on the PV module output power under realistic irradiation," *Energy Procedia*, vol. 92, pp. 523–530, 2016.

[21] K. R. McIntosh *et al.*, "Increase in external quantum efficiency of encapsulated silicon solar cells from a luminescent down-shifting layer," *Prog. Photovoltaics Res. Appl.*, no. 17, pp. 191–197, 2009.

[22] K. R. Mcintosh, J. N. Cotsell, J. S. Cumpston, A. W. Norris, N. E. Powell, and B. M. Ketola, "An optical comparison of silicone and EVA encapsulants for conventional silicon PV modules: A ray-tracing study," in *34th IEEE Photovoltaic Specialists Conference*, 2009, pp. 544–549.